Analysis of the nonlinear stochastic dynamics of an elastic bar with an attached end mass

Americo Cunha Jr, Rubens Sampaio

SEECCM III
3rd South-East European Conference on Computational Mechanics-
an ECCOMAS and IACM Special Interest Conference
M. Papadrakakis, M. Kojic, I. Tuncer (eds.)
Kos Island, Greece, 12–14 June 2013

ANALYSIS OF THE NONLINEAR STOCHASTIC DYNAMICS OF AN ELASTIC BAR WITH AN ATTACHED END MASS

Americo Cunha Jr[1] [2], **Rubens Sampaio**[1]

[1]Department of Mechanical Engineering
Pontifícia Universidade Católica do Rio de Janeiro
Rua Marquês de São Vicente, 225, Gávea, Rio de Janeiro - RJ, Brasil - 22453-900
email: americo.cunhajr@gmail.com rsampaio@puc-rio.br

[2]Laboratory of Multi-Scale Modeling and Simulation
Université Paris-Est Marne-la-Vallée
5, Boulevard Descartes 77454, Marne-la-Vallée Cedex 2, France
email: americo@univ-paris-est.fr

Keywords: nonlinear dynamics, stochastic modeling, maximum entropy principle, uncertainty quantification, Monte Carlo method.

Abstract. *This work studies the nonlinear dynamics of a one-dimensional elastic bar, attached to discrete elements, with viscous damping, random elastic modulus, and subjected to a Gaussian white-noise distributed external force. The system analysis uses the maximum entropy principle to specify the elastic modulus (gamma) probability distribution and uses Monte Carlo simulations to compute the propagation of uncertainty in this discrete–continuous system. After describing the deterministic and the stochastic modeling of the system, some configurations of the model are analyzed in order to characterize the effect of a lumped mass in the overall behavior of this dynamical system. The simulation results show that the system response presents multimodal probability distribution, irregular distribution of energy throughout the spectrum of frequencies, and a limit behavior, for large values of the lumped mass, similar to a mass-spring system.*

1 INTRODUCTION

The dynamics of a mechanical system depends on some parameters such as physical and geometrical properties, constraints, external and internal loading, initial and boundary conditions. Most of the theoretical models used to describe the behavior of a mechanical system assume nominal values for these parameters, such that the model gives one response for a given particular input. In this case the system is *deterministic* and its behavior is described by a single set of differential equations. However, in real systems they do not have a fixed value since they are subjected to uncertainties of measurement, imperfections in manufacturing processes, change of properties, etc. This variability in the set of system parameters leads to a large number of possible system responses for a given particular input. Now the system is *stochastic* and there is a family of differential equations sets (one for each realization of the random parameters) associated to it.

In order to quantify variability of the responses of mechanical systems which are of interest in engineering applications, several recent works have been applying techniques of stochastic modeling, to take into account the inaccuracies due to model and data uncertainty, and uncertainty quantification, to compute the propagation of incertitude of the random parameters through the system. For instance, the reader can see [14, 11, 10], in the context of drillstring dynamics, as well as the work of [19] in hydraulic fracturing. Other studies applying stochastic techniques to describe the random dynamics of flexible structures are [12, 13] and [3]. The analysis of the stochastic dynamics of a highly nonlinear system, with three degrees of freedom, can be seen in [6]. The readers interested in structures built by heterogeneous hyperelastic materials is encouraged to consult [2]. To see the latest theoretical advances of stochastic modeling in structural dynamics, the reader is encouraged to consult the work of [18].

This work aims to conduct a purely theoretical study of the propagation of uncertainty in the dynamics of a nonlinear continuos random system with discrete elements attached to it. This theoretical study aims to illustrate a consistent methodology to analyze the stochastic dynamics of nonlinear mechanical systems. In this sense, this work considers a one-dimensional elastic bar, with random elastic modulus, fixed on the left extreme and with a lumped mass and two springs (one linear and another nonlinear) on the right extreme (fixed-mass-spring bar), subjected to an external force which is proportional to a Gaussian white-noise.

This paper is an extension of work done in [3, 4], which includes additional results and a deeper analysis of the original results. It is organized as follows. Section 2 presents the deterministic modeling of the problem, the discretization procedure and the algorithm used to solve the equation of interest. The stochastic modeling of the problem is shown in section 3, as well as the construction of a probability distribution for the elastic modulus, using the maximum entropy principle, and a brief discussion on the Monte Carlo method. In section 4, some configurations of the model are analyzed in order to characterize the effect of lumped mass in the system dynamical behavior. Finally, in section 5, the main conclusions are emphasized.

2 DETERMINISTIC APPROACH

The system of interest in this study case is the elastic bar fixed at a rigid wall, on the left side, and attached to a lumped mass and two springs (one linear and one nonlinear), on the right side, such as illustrated in Figure 1. From now on, the fixed-mass-spring bar.

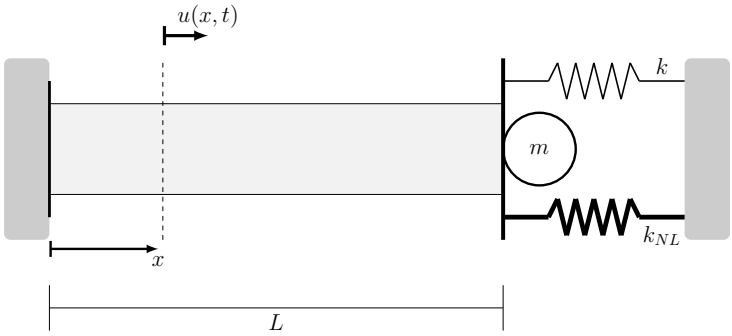

Figure 1: Sketch of a bar fixed at one and attached to two springs and a lumped mass on the other extreme.

2.1 Strong Formulation

The physical quantity of interest is the bar is its displacement field u, which depends on the position x and the time t, and evolves, for all $(x,t) \in (0,L) \times (0,T)$, according to the following partial differential equation

$$\rho A \frac{\partial^2 u}{\partial t^2} + c \frac{\partial u}{\partial t} - \frac{\partial}{\partial x}\left(EA \frac{\partial u}{\partial x} \right) + \left(ku + k_{NL} u^3 + m \frac{\partial^2 u}{\partial t^2} \right) \delta(x-L) = f(x,t), \qquad (1)$$

where ρ is mass density, A is the cross section area, c is the damping coefficient, E is the elastic modulus, k is the stiffness of the linear spring, k_{NL} is the stiffness of the nonlinear spring, m is the lumped mass, and f is a distributed external force, which depends on x and t. The symbol $\delta(x-L)$ denotes the delta of Dirac distribution at $x = L$.

The boundary conditions for this problem are given by

$$u(0,t) = 0, \quad \text{and} \quad EA \frac{\partial u}{\partial x}(L,t) = 0. \qquad (2)$$

The initial position and the initial velocity of the bar are respectively given by

$$u(x,0) = u_0(x), \quad \text{and} \quad \frac{\partial u}{\partial t}(x,0) = v_0(x), \qquad (3)$$

where u_0 and v_0 are known functions of x, defined for $0 \leq x \leq L$.

Moreover, it is noteworthy that u is assumed to be as regular as needed for the initial–boundary value problem of Eqs.(1), (2), and (3) to be well posed.

2.2 Weak Formulation

Let $\mathcal{U}_t$ be the class of (time dependent) basis functions and $\mathcal{W}$ be the class of weight functions. These sets are chosen as the space of functions with square integrable spatial derivative, which satisfy the essential boundary condition defined by Eq.(2).

The weak formulation of the problem under study says that one wants to find $u \in \mathcal{U}_t$ that satisfy, for all $w \in \mathcal{W}$, the weak equation of motion given by

$$\mathcal{M}(\ddot{u}, w) + \mathcal{C}(\dot{u}, w) + \mathcal{K}(u, w) = \mathcal{F}(w) + \mathcal{F}_{NL}(u, w), \qquad (4)$$

where $\mathcal{M}$ is the mass operator, $\mathcal{C}$ is the damping operator, $\mathcal{K}$ is the stiffness operator, $\mathcal{F}$ is the distributed external force operator, and $\mathcal{F}_{NL}$ is the nonlinear force operator. These operators are, respectively, defined as

$$\mathcal{M}(\ddot{u}, w) = \int_0^L \rho A \ddot{u}(x,t) w(x) dx + m \ddot{u}(L,t) w(L), \tag{5}$$

$$\mathcal{C}(\dot{u}, w) = \int_0^L c \dot{u}(x,t) w(x) dx, \tag{6}$$

$$\mathcal{K}(u, w) = \int_0^L EA u'(x,t) w'(x) dx + k u(L,t) w(L), \tag{7}$$

$$\mathcal{F}(w) = \int_0^L f(x,t) w(x) dx, \tag{8}$$

$$\mathcal{F}_{NL}(u, w) = -k_{NL} \left(u(L,t)\right)^3 w(L), \tag{9}$$

where $\dot{}$ is an abbreviation for temporal derivative and $'$ is an abbreviation for spatial derivative.

The weak formulations for the initial conditions of Eq.(3), which are valid for all $w \in \mathcal{W}$, are respectively given by

$$\widetilde{\mathcal{M}}(u(\cdot,0), w) = \widetilde{\mathcal{M}}(u_0, w), \tag{10}$$

and

$$\widetilde{\mathcal{M}}(\dot{u}(\cdot,0), w) = \widetilde{\mathcal{M}}(v_0, w), \tag{11}$$

where $\widetilde{\mathcal{M}}$ is the associated mass operator, defined as

$$\widetilde{\mathcal{M}}(u, w) = \int_0^L \rho A u(x,t) w(x) dx. \tag{12}$$

2.3 Galerkin Formulation

To approximate the solution of the variational problem given by Eqs.(4) to (11), the Galerkin method [5] is employed, which approximates the displacement field u by a linear combination of the form

$$u(x,t) \approx \sum_{n=1}^{N} u_n(t) \phi_n(x), \tag{13}$$

where the basis functions ϕ_n are the orthogonal modes of the conservative and non-forced dynamical system associated to the fixed-mass-spring bar, and the coefficients u_n are time-dependent functions. This results in the following system of ordinary differential equations

$$[M]\, \ddot{\mathbf{u}}(t) + [C]\, \dot{\mathbf{u}}(t) + [K]\, \mathbf{u}(t) = \mathbf{f}(t) + \mathbf{f}_{NL}\left(\dot{\mathbf{u}}(t)\right), \tag{14}$$

supplemented by the following pair of initial conditions

$$\mathbf{u}(0) = \mathbf{u}_0 \qquad \text{and} \qquad \dot{\mathbf{u}}(0) = \mathbf{v}_0, \tag{15}$$

where $\mathbf{u}(t)$ is the vector of $\mathbb{R}^N$ in which the n-th component is the $u_n(t)$, $[M]$ is the mass matrix, $[C]$ is the damping matrix, $[K]$ is the stiffness matrix. Also, $\mathbf{f}(t)$, $\mathbf{f}_{NL}\left(\mathbf{u}(t)\right)$, $\mathbf{u}_0$, and $\mathbf{v}_0$ are vectors of $\mathbb{R}^N$, which respectively represent the external force, the nonlinear force, the initial position, and the initial velocity. The initial value problem of Eqs.(14) and (15) has its solution approximated by Newmark method [5].

3 STOCHASTIC APPROACH

3.1 Probabilistic Model

Consider a probability space $(\Theta, \mathbb{A}, \mathbb{P})$, where Θ is sample space, $\mathbb{A}$ is a σ-field over Θ and $\mathbb{P}$ is a probability measure. In this probabilistic space, the elastic modulus is assumed to be a random variable $E : \Theta \to \mathbb{R}$ that associates to each event $\theta \in \Theta$ a real number $E(\theta)$. Also, the distributed external force acting on the system is given by the random field $F : [0, L] \times [0, T] \times \Theta \to \mathbb{R}$ such that

$$F(x, t, \theta) = \sigma \phi_1(x) N(t, \theta), \tag{16}$$

where σ is the force amplitude, and $N(t, \theta)$ is a Gaussian white-noise with zero mean and unit variance. A white-noise is a random process which all instants of time are uncorrelated. In other words, the behavior of the process at any given instant of time has no influence on the other instants. A typical realization of the random external force, given by Eq.(16), for fixed position, is shown in Figure 2.

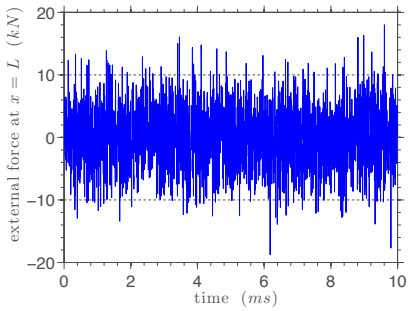

Figure 2: This figure illustrates a realization of the random external force.

3.2 Elastic Modulus Distribution

The elastic modulus cannot be negative, so it is reasonable to assume the support of random variable E as the interval $(0, \infty)$. Therefore, the probability density function (PDF) of E is a nonnegative function $p_E : (0, \infty) \to \mathbb{R}$, which respects the following normalization condition

$$\int_0^\infty p_E(\xi) d\xi = 1. \tag{17}$$

Also, the mean value of E is known real number μ_E, i.e.,

$$\mathbb{E}\left[E\right] = \mu_E, \tag{18}$$

where the expected value operator of E is defined as

$$\mathbb{E}\left[E\right] = \int_0^\infty E(\xi) p_E(\xi) d\xi \tag{19}$$

Finally, one also wants E to have a finite variance, i.e.,

$$\mathbb{E}\left[\left(E - \mu_E\right)^2\right] < \infty, \tag{20}$$

which is possible [17], for example, if

$$\mathbb{E}\left[\ln\left(E\right)\right] < \infty. \tag{21}$$

Following the suggestion of [17], the maximum entropy principle is employed in order to consistently specify p_E. This methodology chooses for E the PDF which maximizes the differential entropy function, defined by

$$\mathbb{S}\left[p_E\right] = -\int_0^\infty p_E(\xi) \ln\left(p_E(\xi)\right) d\xi, \tag{22}$$

subjected to (17), (18), and (21), the restrictions that effectively define the known information about E.

Respecting the constraints imposed by (17), (18), and (21), the PDF that maximizes Eq.(22) is given by

$$p_E(\xi) = \mathbb{1}_{(0,\infty)} \frac{1}{\mu_E} \left(\frac{1}{\delta_E^2}\right)^{\left(\frac{1}{\delta_E^2}\right)} \frac{1}{\Gamma(1/\delta_E^2)} \left(\frac{\xi}{\mu_E}\right)^{\left(\frac{1}{\delta_E^2} - 1\right)} \exp\left(-\frac{\xi}{\delta_E^2 \mu_E}\right), \tag{23}$$

where $\mathbb{1}_{(0,\infty)}$ denotes the indicator function of the interval $(0,\infty)$, δ_E is the dispersion factor of E, and Γ indicates the gamma function. This PDF characterizes a gamma distribution.

3.3 Stochastic Equation of Motion

As a consequence of the randomness of F and E, the displacement of the bar becomes a random field $U : [0, L] \times [0, T] \times \Theta \to \mathbb{R}$, which evolves according the following stochastic partial differential equation

$$\rho A \frac{\partial^2 U}{\partial t^2} + c \frac{\partial U}{\partial t} - \frac{\partial}{\partial x}\left(EA \frac{\partial U}{\partial x}\right) + \left(kU + k_{NL} U^3 + m \frac{\partial^2 U}{\partial t^2}\right) \delta(x - L) = F(x, t, \theta), \tag{24}$$

being the partial derivatives now defined in the mean square sense [9]. This problem has boundary and initial conditions similar to those defined in Eqs.(2) and (3), by changing u for U only.

3.4 Stochastic Solver: Monte Carlo Method

Uncertainty propagation in the stochastic dynamics of the discrete–continuous system under study is computed by Monte Carlo (MC) method [7, 16, 15]. This stochastic solver uses a Mersenne twister pseudorandom number generator [8], to obtain many realizations of E and F. Each one of these realizations defines a new Eq.(4), so that a new weak problem is obtained. After that, these new weak problems are solved deterministically, such as in section 2.3. All the MC simulations reported in this work use 4096 samples to access the random system.

4 NUMERICAL EXPERIMENTS

The numerical experiments presented in this section adopt the following deterministic parameters for the studied system: $\rho = 7900\ kg/m^3$, $c = 5\ kNs/m$, $A = 625\pi\ mm^2$, $k = 650\ N/m$, $k_{NL} = 650 \times 10^{13}\ N/m^3$, $L = 1\ m$, $\sigma = 5\ kN$ and $T = 10\ ms$. The random variable E, is characterized by $\mu_E = 203\ GPa$ and $\delta_E = 10\%$. The initial conditions for displacement and velocity are respectively given by

$$u_0(x) = \alpha_1 \phi_3(x) + \alpha_2 x, \qquad \text{and} \qquad v_0(x) = 0, \tag{25}$$

where $\alpha_1 = 0.1\ mm$ and $\alpha_2 = 0.5 \times 10^{-3}$. Note that u_0 reaches the maximum value at $x = L$. This function is used to "activate" the spring cubic nonlinearity, which depends on the displacement at $x = L$. A parametric study, with $m^* = 0.1,\ 1,\ 10,\ 50$, is performed to investigate the effect of the end mass on the bar dynamics, where the discrete–continuous mass ratio is defined as

$$m^* = \frac{m}{\rho A L}. \tag{26}$$

4.1 Displacement, Velocity, and Phase Space

The mean value of displacement $U(L, \cdot, \cdot)$ and an envelope of reliability, wherein a realization of the stochastic system has 98% of probability of being contained, are shown, for different values of m^*, in Figure 3. By observing this figure one can note that, as the value of lumped mass increases, the decay of the system displacement amplitude decreases significantly. This indicates that this system is not much influenced by damping for large values of m^*.

Furthermore, for all values of m^*, the amplitude of the confidence interval increases with time. This indicates that the uncertainty of the system is greater in the stationary regime. This greater uncertainty in the stationary response of the system is due to white-noise forcing. As the initial conditions do not affect the steady state, the response in this regime is subjected to greater variability. This statement can also be checked if the reader look at Figure 4, which shows information similar to the one presented in Figure 3, but now for velocity $\dot{U}(L, \cdot, \cdot)$.

The mean phase space of the fixed-mass-spring bar at $x = L$ is shown, for different values of m^*, in Figure 5. The observation made in the previous paragraphs can be confirmed by analyzing this figure, since the system mean orbit tends from a stable focus to an ellipse as m^* increases. In other words, the limiting behavior of the system when $m^* \to \infty$ is a mass-spring system.

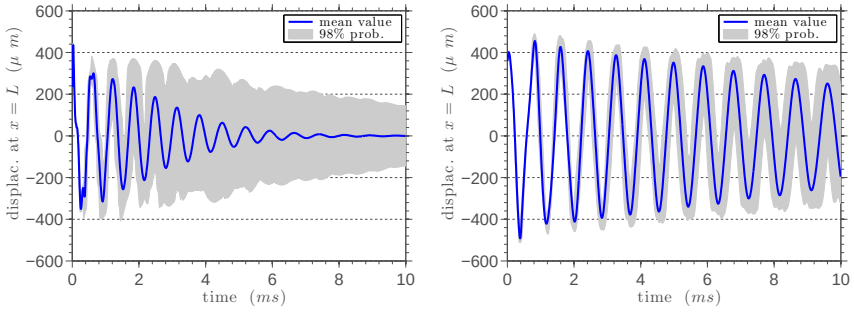

(a) $m^* = 0.1$ (b) $m^* = 1$

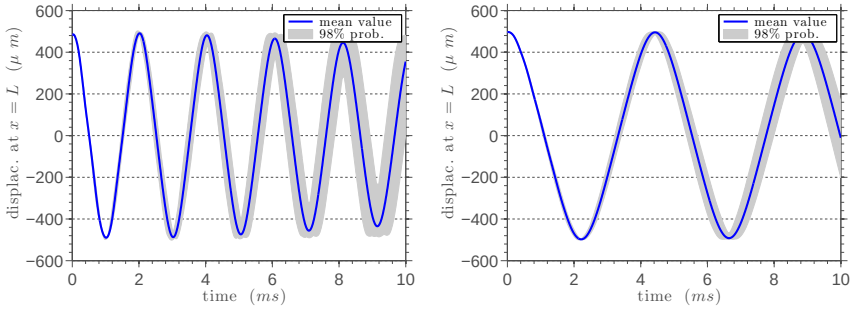

(c) $m^* = 10$ (d) $m^* = 50$

Figure 3: This figure illustrates the mean value (blue line) and a 98% of probability interval of confidence (grey shadow) for the random process $U(L, \cdot, \cdot)$, for several values of the discrete–continuous mass ratio.

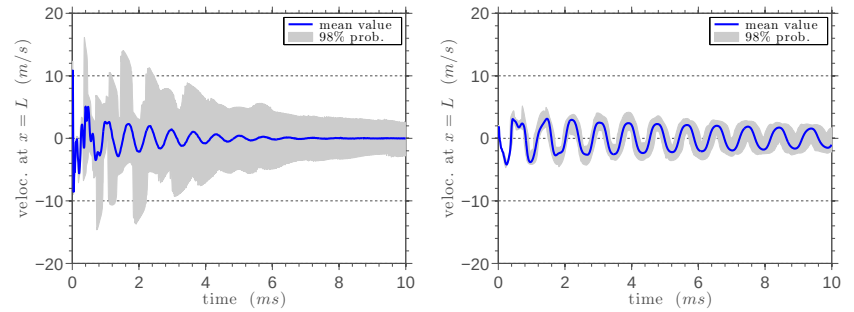

(a) $m^* = 0.1$ (b) $m^* = 1$

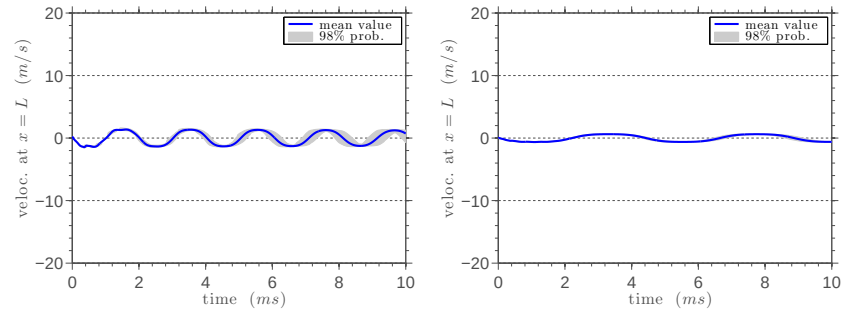

(c) $m^* = 10$ (d) $m^* = 50$

Figure 4: This figure illustrates the mean value (blue line) and a 98% of probability interval of confidence (grey shadow) for the random process $\dot{U}(L, \cdot, \cdot)$, for several values of the discrete–continuous mass ratio.

This limit behavior, which tends to a conservative system, occurs because, with the increasing of m^*, most of the mass of the system becomes concentrated at the right extreme of the bar. Thus, the bar behaves like a massless spring. Also, as the damping is distributed along the bar and the mass of it became negligible, the viscous dissipation becomes ineffective.

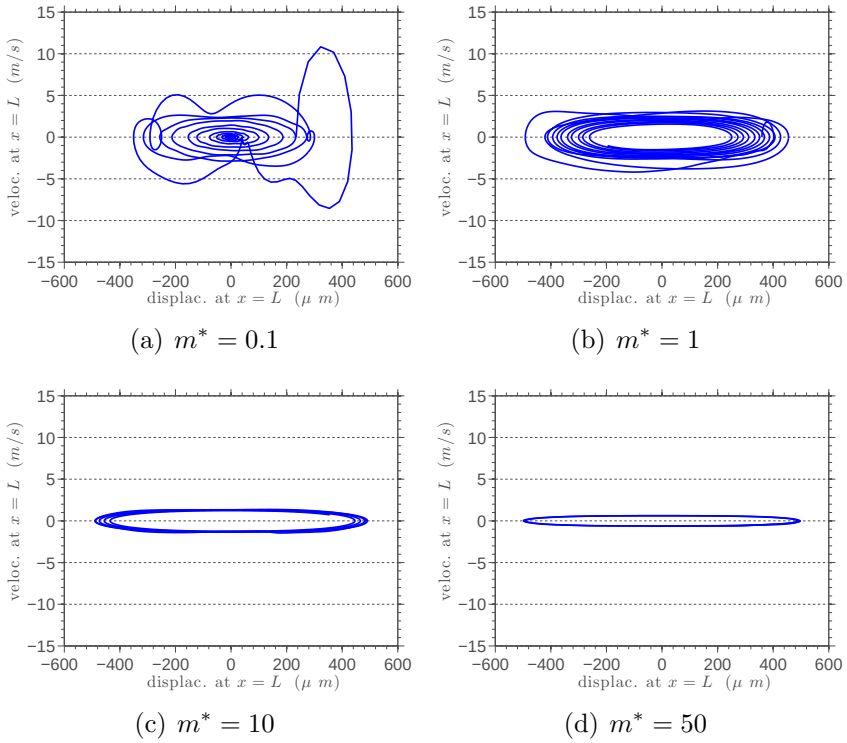

(a) $m^* = 0.1$ (b) $m^* = 1$

(c) $m^* = 10$ (d) $m^* = 50$

Figure 5: This figure illustrates the mean value of the fixed-mass-spring bar phase space at $x = L$, for several values of the discrete–continuous mass ratio.

4.2 Probability Density Function

The difference between the system dynamical behavior, for different values of m^*, is even clearer if one looks to the PDF estimations[1] of the normalized[2] random variable $U(L, T, \cdot)$, which are presented in Figure 6.

For $m^* = 0.1$, the distribution is approximately symmetric around the mean, with three modes. The central mode slightly displaced to the left of the mean. The other two modes are symmetrical around the first mode. This symmetry implies in a symmetrical behavior around the mean for the displacement at $(x, t) = (L, T)$, that can be observed in Figure 3.

On the other hand, when $m^* = 1$ or 10 the distribution still is multimodal, however asymmetrical around the mean. This asymmetry implies that the most frequent value of the realizations is not the mean value. Note in the Figure 3 that the displacements are not uniformly distributed around the mean.

[1] These estimates were obtained using a kernel smooth density technique [1].

[2] In this context normalized means a random variable with zero mean and unit standard deviation.

Furthermore, it can be noted that, when $m^* = 50$, the distribution is unimodal and approximately symmetrical around the mean. Thus, the greatest probability occurs around the mean value of $U(L, T, \cdot)$. Thus, the dispersion around the mean is very small, which can be verified in the confidence interval shown in Figure 3.

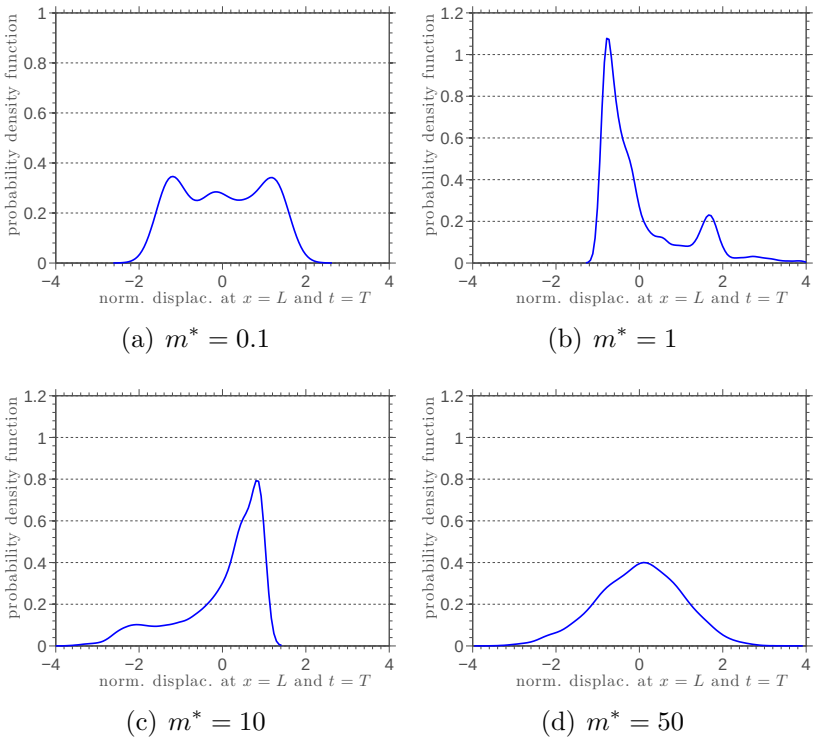

(a) $m^* = 0.1$ (b) $m^* = 1$

(c) $m^* = 10$ (d) $m^* = 50$

Figure 6: This figure illustrates estimations to the PDF of the (normalized) random variable $U(L, T, \cdot)$, for several values of the discrete–continuous mass ratio.

4.3 Power Spectral Density

The energy distribution of the bar through the frequency spectrum can be seen in Figure 7, which shows the power spectral density (PSD) function of the bar velocity at $x = L$.

It may be noted that, when the value of m^* is changed, the energy is irregular redistributed along the spectrum of frequencies. This behavior can be explained by the presence of the spring cubic nonlinearity, and by the white-noise forcing, that excites the mechanical system at all frequencies of the spectrum.

Also, it can be noted that, large values of m^* have a greater number of peaks in higher frequencies. However, in all cases analyzed, the peaks with greater height, and thus, the more energy, appears at the lower frequencies of the spectrum.

5 CONCLUDING REMARKS

This work presents a model to describe the nonlinear dynamics of a elastic bar, attached to discrete elements, with viscous damping, random elastic modulus, and subjected to a Gaussian white-noise distributed external force is presented. The elastic modulus is modeled as a random variable with gamma distribution, being the probability distribution of this parameter obtained by the use of the maximum entropy principle.

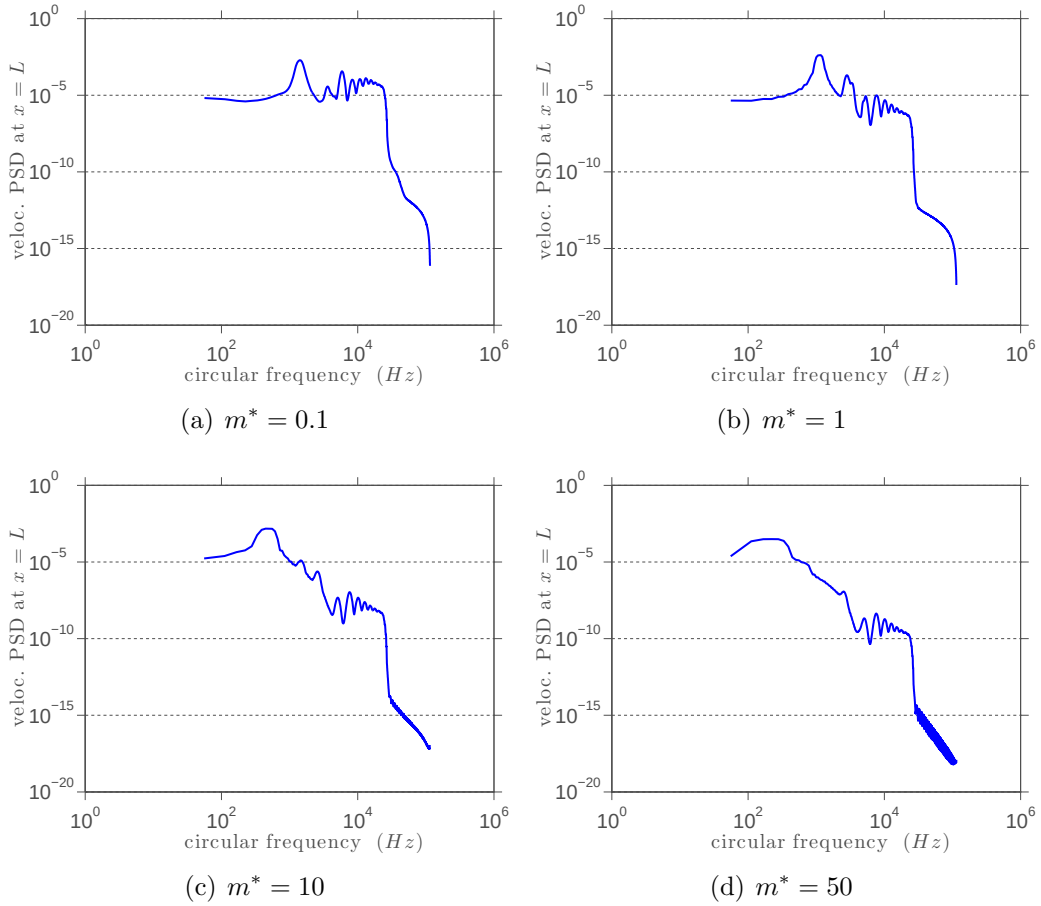

(a) $m^* = 0.1$ (b) $m^* = 1$

(c) $m^* = 10$ (d) $m^* = 50$

Figure 7: This figure illustrates estimations to the PSD of the random process $\dot{U}(L, \cdot, \cdot)$, for several values of the discrete–continuous mass ratio.

Several configurations of the model are analyzed in to order to characterize the effect of the lumped mass in the overall behavior of the random dynamical system. This analysis shows that the dynamics of the random system is significantly altered when the values of the lumped mass are varied. It is observed that this system behaves, in the limiting case where the lumped mass is very large, such as a spring mass system. Furthermore, it can be noticed probability distributions for the bar displacement with multimodal behavior, and an irregular redistribution of energy in the power spectrum of velocity.

ACKNOWLEDGMENTS

The authors are indebted to Brazilian Council for Scientific and Technological Development (CNPq), Coordination of Improvement of Higher Education Personnel (CAPES), and Foundation for Research Support in Rio de Janeiro State (FAPERJ) for the financial support given to this research.

REFERENCES

[1] A. W. Bowman and A. Azzalini. *Applied Smoothing Techniques for Data Analysis*. Oxford University Press, New York, 1997.

[2] A. Clément, C. Soize, and J. Yvonnet. Uncertainty quantification in computational

stochastic multiscale analysis of nonlinear elastic materials. *Computer Methods in Applied Mechanics and Engineering*, 254:61–82, 2013.

[3] A. Cunha Jr and R. Sampaio. Effect of an attached end mass in the dynamics of uncertainty nonlinear continuous random system. *Mecánica Computacional*, 31:2673–2683, 2012.

[4] A. Cunha Jr and R. Sampaio. Uncertainty propagation in the dynamics of a nonlinear random bar. In *Proceedings of the XV International Symposium on Dynamic Problems of Mechanics*, 2013.

[5] T. J. R. Hughes. *The Finite Element Method*. Dover Publications, New York, 2000.

[6] R. Q. Lima and R. Sampaio. Stochastic analysis of an electromechanical coupled system with embarked mass. *Mecánica Computacional*, 31:2783–2800, 2012.

[7] Jun S. Liu. *Monte Carlo Strategies in Scientific Computing*. Springer, New York, 2001.

[8] M. Matsumoto and T. Nishimura. Mersenne twister: a 623-dimensionally equidistributed uniform pseudo-random number generator. *ACM Transactions on Modeling and Computer Simulation*, 8:3–30, 1998.

[9] A. Papoulis and S. U. Pillai. *Probability, Random Variables and Stochastic Processes*. McGraw-Hill, New- York, 4th edition, 2002.

[10] T. G. Ritto, M. R. Escalante, R. Sampaio, and M. B. Rosales. Drill-string horizontal dynamics with uncertainty on the frictional force. *Journal of Sound and Vibration*, 332:145–153, 2013.

[11] T. G. Ritto and R. Sampaio. Stochastic drill-string dynamics with uncertainty on the imposed speed and on the bit-rock parameters. *International Journal for Uncertainty Quantification*, 2:111–124, 2012.

[12] T. G. Ritto, R. Sampaio, and E. Cataldo. Timoshenko beam with uncertainty on the boundary conditions. *Journal of the Brazilian Society of Mechanical Sciences and Engineering*, 30:295–303, 2008.

[13] T. G. Ritto, R. Sampaio, and F. Rochinha. Model uncertainties of flexible structures vibrations induced by internal flows. *Journal of the Brazilian Society of Mechanical Sciences and Engineering*, 33:373–380, 2011.

[14] T. G. Ritto, C. Soize, and R. Sampaio. Non-linear dynamics of a drill-string with uncertain model of the bit rock interaction. *International Journal of Non-Linear Mechanics*, 44:865–876, 2009.

[15] C. P. Robert and G. Casella. *Monte Carlo Statistical Methods*. Springer, New York, 2010.

[16] R. W. Shonkwiler and F. Mendivil. *Explorations in Monte Carlo Methods*. Springer, New York, 2009.

[17] C. Soize. A nonparametric model of random uncertainties for reduced matrix models in structural dynamics. *Probabilistic Engineering Mechanics*, 15:277 – 294, 2000.

[18] C. Soize. Stochastic modeling of uncertainties in computational structural dynamics - recent theoretical advances. *Journal of Sound and Vibration*, 332:2379—2395, 2013.

[19] S. Zio and F. Rochinha. A stochastic collocation approach for uncertainty quantification in hydraulic fracture numerical simulation. *International Journal for Uncertainty Quantification*, 2:145–160, 2012.